Causal links between gut microbiota, metabolites, and diffuse large B-cell lymphoma: Evidence from a Mendelian randomization study

Ganyu Feng[1,A–D], Guangcai Zhong[1,A,B], Cong Wang[1,B], Ran Kong[1,B], *Jianhong Wang[1,A,E], *Xiangxiang Zhou[1,2,A,E,F]

[1] Department of Hematology, Shandong Provincial Hospital Affiliated to Shandong First Medical University, Jinan, China
[2] Department of Hematology, Shandong Provincial Hospital, Shandong University, Jinan, China

A – research concept and design; B – collection and/or assembly of data; C – data analysis and interpretation;
D – writing the article; E – critical revision of the article; F – final approval of the article

Advances in Clinical and Experimental Medicine, ISSN 1899–5276 (print), ISSN 2451–2680 (online) *Adv Clin Exp Med*. 2026;35(5):877–888

Address for correspondence
Xiangxiang Zhou
E-mail: xiangxiangzhou@sdu.edu.cn

Funding sources
None declared

Conflict of interest
None declared

*Jianhong Wang and Xiangxiang Zhou contributed equally to this work.

Received on March 9, 2025
Reviewed on May 19, 2025
Accepted on July 28, 2025

Published online on March 25, 2026

Cite as
Feng G, Zhong G, Wang C, Kong R, Wang J, Zhou X. Causal links between gut microbiota, metabolites, and diffuse large B-cell lymphoma: Evidence from a Mendelian randomization study. *Adv Clin Exp Med*. 2026;35(5):877–888. doi:10.17219/acem/208704

DOI
10.17219/acem/208704

Abstract

Background. The precise causal relationship between alterations in the gut microbiota, microbiota-derived metabolites, and the development of diffuse large B-cell lymphoma (DLBCL) remains unclear.

Objectives. To investigate the potential causal relationships between gut microbiota, microbiota-derived metabolites, and DLBCL.

Materials and methods. Genetic data on gut microbiota were obtained from the MiBioGen consortium, while data on microbiota-derived metabolites were sourced from the TwinsUK and KORA studies. Summary statistics for DLBCL were retrieved from FinnGen. Mendelian randomization (MR) analysis was performed, with inverse-variance weighting (IVW) used as the primary analytical method. Sensitivity analyses included Cochran's Q test, the MR-Egger intercept test, and MR-PRESSO. Reverse MR analysis was conducted to assess potential bidirectional causal relationships between gut microbiota and DLBCL. Bayesian weighted MR (BWMR) was applied for additional validation to enhance the robustness of the findings.

Results. Among 196 gut microbial taxa analyzed, *Bilophila* (odds ratio (OR) = 1.777, 95% confidence interval (95% CI): 1.053–3.000, p = 0.031) was associated with an increased risk of DLBCL. In contrast, *Alistipes* (OR = 0.521, 95% CI: 0.311–0.873, p = 0.013) and *Ruminococcaceae* UCG011 (OR = 0.749, 95% CI: 0.574–0.978, p = 0.034) were associated with a reduced risk. Reverse MR analysis demonstrated a positive association between DLBCL risk and the abundance of *Anaerofilum* (OR = 1.087, 95% CI: 1.008–1.173, p = 0.031). Negative associations were observed between DLBCL risk and the abundance of Deltaproteobacteria (OR = 0.959, 95% CI: 0.922–0.997, p = 0.037), *Desulfovibrionales* (OR = 0.959, 95% CI: 0.922–0.998, p = 0.041), Oxalobacteraceae (OR = 0.914, 95% CI: 0.843–0.992, p = 0.031), and *Oxalobacter* (OR = 0.909, 95% CI: 0.837–0.988, p = 0.024). Analysis of microbiota-derived metabolites identified a causal association between indolepropionate (OR = 0.296, 95% CI: 0.131–0.669, p = 0.003) and reduced DLBCL risk, whereas 7-alpha-hydroxy-3-oxo-4-cholestenoate (7-HOCA) (OR = 9.561, 95% CI: 1.426–64.088, p = 0.020) was associated with an increased risk. No evidence of directional pleiotropy or heterogeneity was detected.

Conclusions. This MR study provides evidence that specific gut microbial taxa and microbiota-derived metabolites may causally influence the risk of DLBCL.

Key words: metabolomics, gut microbiota, diffuse large B-cell lymphoma, Mendelian randomization, Bayesian statistics

Highlights

- Mendelian randomization identifies causal associations between gut microbiota, microbial metabolites, and diffuse large B-cell lymphoma (DLBCL) risk.
- *Alistipes* and *Ruminococcaceae* UCG011 are inversely associated with DLBCL, whereas *Bilophila* increases disease risk.
- The microbial metabolite indolepropionate shows protective effects against DLBCL, while 7-HOCA is positively associated with lymphoma development.
- Evidence supports bidirectional interactions between DLBCL and specific gut bacterial taxa.

Background

Non-Hodgkin lymphoma (NHL) comprises a heterogeneous group of malignant lymphoproliferative disorders arising from lymphocytes.[1] In recent decades, the incidence of NHL has increased significantly, and it now ranks as the 11th most common malignancy worldwide, contributing substantially to the global cancer burden.[1,2] Diffuse large B-cell lymphoma (DLBCL) is the most prevalent subtype of NHL, accounting for approx. 30–58% of cases, with notable geographic variation in its distribution.[3,4]

Although DLBCL is considered clinically aggressive, standard treatment regimens generally yield favorable outcomes, with 60–70% of patients achieving a 5-year overall survival (OS) rate. Nevertheless, approx. 30–40% of patients eventually experience relapse or treatment failure, partly due to an incomplete understanding of the disease's underlying pathogenic mechanisms.[3]

Although the etiology of DLBCL remains incompletely elucidated, accumulating evidence suggests its development involves complex interactions between genetic susceptibility, immune dysregulation, and environmental exposures.[5] In this context, the proposed microbiota–gut–lymphoma axis highlights the potential mechanistic link between microbial alterations and lymphomagenesis.[6,7] The human gastrointestinal tract contains approx. 100 trillion microorganisms,[8,9] which contribute to host physiology by enhancing nutrient absorption,[10] providing pathogen defense,[11] maintaining intestinal barrier function, modulating epithelial differentiation,[12] and regulating immune responses.[13] However, disruption of these microbial communities, referred to as dysbiosis, may impair normal physiological functions.[9] Characterized by a reduction in beneficial microbes and/or an increase in pathogenic species, dysbiosis has been linked to chronic inflammation, immune dysregulation, and tumor development.[7,14] Emerging evidence indicates that the gut microbiota contributes not only to the development of gastrointestinal malignancies but also to oncogenesis at extraintestinal sites.[14–19] Recent studies have identified distinct gut microbial profiles in newly diagnosed DLBCL patients compared with healthy controls,[18,20–22] with specific alterations in microbial composition correlating with clinical outcomes.[22,23] Furthermore, accumulating evidence indicates that microbial metabolites may influence DLBCL progression by modulating immunometabolic pathways.[24]

Although current research has demonstrated correlations between gut microbial profiles, microbial metabolites, and DLBCL, causal relationships remain unproven, as most existing studies have employed case–control designs and therefore cannot establish temporal relationships between microbial alterations and lymphomagenesis.[22] In addition, observational studies examining gut microbiota–DLBCL associations are subject to inherent limitations due to multiple confounding factors, including age, environmental exposures, diet, lifestyle, comorbidities, and therapeutic interventions, which may substantially bias association estimates.[25] While randomized controlled trials represent the gold standard for causal inference, their implementation is often limited by ethical and practical constraints. Therefore, Mendelian randomization (MR) and other causal inference methodologies may offer alternative approaches to elucidate potential microbiome–lymphoma relationships. Mendelian randomization is an epidemiological method that strengthens causal inference by using genetic variants as instrumental variables (IVs), leveraging the random allocation of alleles at conception to minimize confounding from postnatal environmental factors.[26] This approach has gained increasing utility in investigating potential causal links between gut microbiota composition and various cancers.[27,28]

This study employed a two-sample MR framework to systematically investigate potential causal relationships between gut microbiota composition and DLBCL risk. We aimed to elucidate the role of specific gut microbial taxa in DLBCL pathogenesis while simultaneously assessing the bidirectional nature of microbiota–lymphoma associations. Furthermore, we evaluated potential causal relationships between gut microbiota–derived metabolites and DLBCL development. By applying robust MR methodologies, our findings may provide novel insights into gut microbiome–DLBCL interactions and potentially inform the development of microbiota-targeted strategies for DLBCL prevention and clinical management.

Objectives

This study employed MR to systematically investigate causal relationships between gut microbiota composition and DLBCL risk, with a particular focus on identifying potentially pathogenic microbial taxa and their contributions to DLBCL lymphomagenesis. Our findings may provide insights into the development of microbiome-modulating interventions for DLBCL prevention and treatment.

Materials and methods

Study design

This MR study was conducted in accordance with the Epidemiology-MR (STROBE-MR) guidelines. We applied both conventional two-sample MR and Bayesian weighted MR (BWMR) to assess causal relationships between gut microbiota composition, microbial metabolites, and DLBCL risk. A schematic overview of the study design is presented in Fig. 1. Instrumental variables were selected as single nucleotide polymorphisms (SNPs) significantly associated with the exposures from genome-wide association study (GWAS) datasets. Mendelian randomization analyses were performed using the TwoSampleMR package in the R statistical environment (R Foundation for Statistical Computing, Vienna, Austria). Comprehensive sensitivity analyses, including heterogeneity tests, pleiotropy assessments, and leave-one-out analyses, were conducted to evaluate the robustness of the findings. In addition, BWMR provided further validation of the causal estimates through its robust Bayesian framework. Reverse MR analyses were also performed to evaluate potential reverse causality between gut microbiota and DLBCL. Our analytical framework satisfied the 3 core assumptions of MR:

1. The SNPs used as IVs must be robustly associated with the exposure;
2. The IVs must be independent of confounders influencing both the exposure and the outcome;
3. The IVs must affect the outcome exclusively through the exposure (i.e., absence of horizontal pleiotropy).

Data sources

The gut microbiota dataset was obtained from the MiBioGen consortium GWAS (https://mibiogen.gcc.rug.nl), comprising 18,340 individuals of predominantly European ancestry across 24 cohorts.[29] This resource provided 16S rRNA gene sequencing profiles paired with genome-wide genotyping data, identifying 211 bacterial taxa across 5 taxonomic levels: 9 phyla, 16 classes, 20 orders, 35 families, and 131 genera. To enhance analytical robustness, we excluded 3 taxonomically undefined families and 12 unclassified genera that could introduce annotation

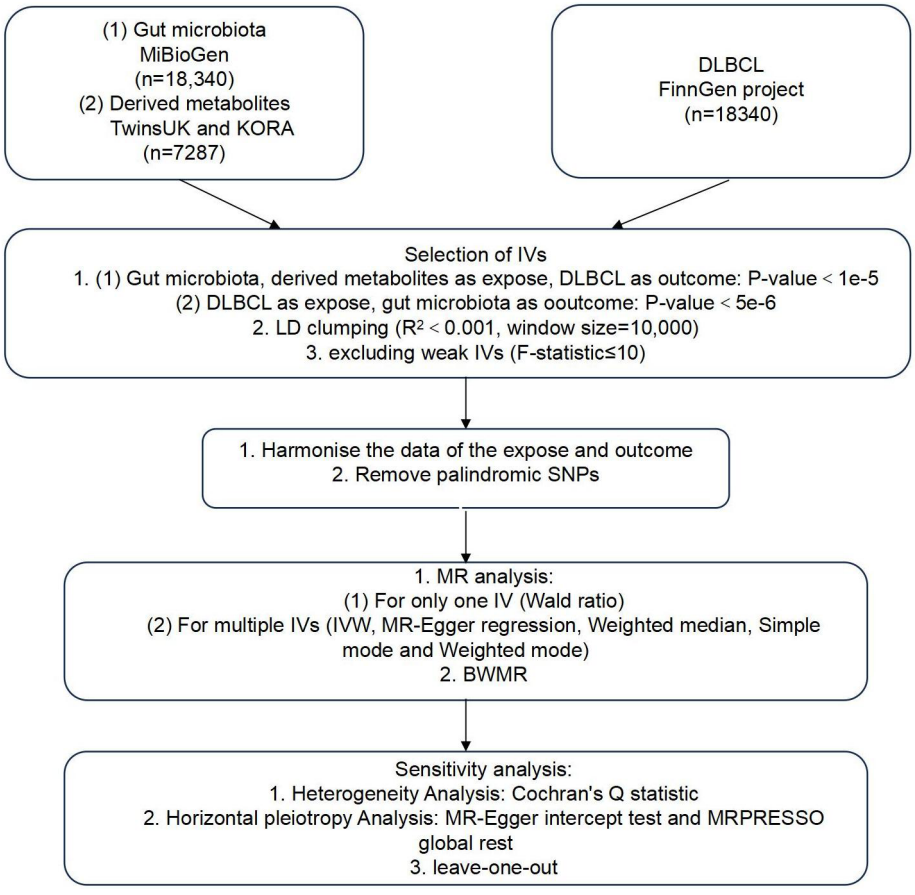

Fig. 1. Flowchart of the Mendelian randomization (MR) analysis investigating the associations between gut microbiota, microbiota-derived metabolites, and diffuse large B-cell lymphoma (DLBCL)

inconsistencies or noise into SNP-exposure associations. Metabolite GWAS data were obtained from 2 European population-based studies (TwinsUK and KORA), comprising 7,824 participants with quantitative profiles of 486 circulating metabolites. From this dataset, we systematically identified and extracted 77 gut microbiota-derived metabolites through annotation based on the Human Metabolome Database (https://hmdb.ca).

The DLBCL summary statistics were obtained from the latest release (R10; published December 18, 2023) of the FinnGen consortium, specifically from the "Diffuse large B-cell lymphoma" dataset, comprising 1,050 cases and 314,193 controls. As this study exclusively utilized de-identified, publicly available data from established consortia, no additional institutional ethics approval was required. When treating gut microbiota and their derived metabolites as exposures and DLBCL as the outcome, the selection of IVs was based on the following criteria: 1) Based on prior literature, we set the significance threshold at $p < 1.0 \times 10^{-5}$ to maximize the number of genetic instruments for exposures[30]; 2) To ensure independence between IVs, LD pruning was conducted using a threshold of $r^2 < 0.001$ and a clumping window of 10,000 kb[30]; 3) Exposure and outcome datasets were harmonized, with palindromic SNPs removed. Single nucleotide polymorphisms with F-statistics ≤10 were excluded to ensure instrument strength, as the F-statistic reflects the strength of the association between IVs and the exposure.[31] For the reverse MR, in which DLBCL was treated as the exposure and gut microbiota as the outcome, the significance threshold was set at $p < 5 \times 10^{-6}$. All other IV selection criteria were consistent with those applied in the forward MR analysis.

Statistical analyses

A range of MR methodologies was applied to investigate the potential causal association between gut microbiota and DLBCL. For bacterial genera with only a single available IV, the Wald ratio method was used to estimate causal effects.[32] When multiple IVs were available, 5 complementary MR methods were applied: inverse-variance weighted (IVW), MR-Egger regression, weighted median, simple mode, and weighted mode. Under the assumption of no horizontal pleiotropy, the IVW method provides the most precise estimates and was therefore selected as the primary analytical approach in this study.[33] MR-Egger regression, which assumes that instrument strength is independent of direct effects (InSIDE assumption), was used as a sensitivity analysis to assess horizontal pleiotropy.[34] The weighted median method can provide consistent causal estimates even when up to 50% of the genetic instruments are invalid.[35] A key excerpt of the R script used for the data analysis is provided in the shared raw data. The F-statistic for each SNP was calculated using the formula $F = \beta^2/SE^2$, and SNPs with F-statistics ≤10 were excluded to minimize weak instrument bias. To assess the robustness of MR estimates, several sensitivity analyses were subsequently performed. Cochran's Q test was used to detect heterogeneity among IVs, with $p < 0.05$ indicating statistical significance.[36] Horizontal pleiotropy was evaluated using both the MR-Egger intercept test (estimating the average pleiotropic effect) and the MR-PRESSO global test (detecting outlier SNPs).[34,37] In addition, a leave-one-out analysis was conducted to determine whether any single IV had a disproportionate influence on causal effect estimates.[38] The BWMR was employed to account for uncertainties arising from polygenicity and to address violations of IV assumptions by controlling for outliers.[39]

Results

MR results

The IVW method was used as the primary analytical approach, with BWMR providing complementary validation. The IVW analysis identified 4 gut microbial taxa showing statistically significant associations with DLBCL risk ($p < 0.05$). Specifically, *Bilophila* (odds ratio (OR) = 1.777, 95% confidence interval (95% CI): 1.053–3.000, p = 0.031) and Desulfovibrionaceae (OR = 1.577, 95% CI: 1.003–2.487, p = 0.049) were positively associated with an increased risk of DLBCL. In contrast, *Alistipes* (OR = 0.521, 95% CI: 0.311–0.873, p = 0.013) and *Ruminococcaceae* UCG011 (OR = 0.749, 95% CI: 0.574–0.978, p = 0.034) were inversely associated with DLBCL risk (Table 1). Scatter plots illustrating the nominally significant associations ($p < 0.05$) identified through IVW analysis are presented in Fig. 2A–C.

The BWMR validation confirmed 3 of these associations and refined their effect estimates. *Alistipes* (OR = 0.573, 95% CI: 0.341–0.964; p = 0.036) and *Ruminococcaceae* UCG011 (OR = 0.747, 95% CI: 0.565–0.987; p = 0.040) maintained their inverse associations with DLBCL risk, whereas *Bilophila* demonstrated a stronger positive association (OR = 2.005, 95% CI: 1.238–3.248; p = 0.005). In contrast, the association for Desulfovibrionaceae was no longer statistically significant in the BWMR analysis (OR = 1.342, 95% CI: 0.846–2.130; p = 0.212), and was therefore not considered in subsequent analyses (Table 1).

Moreover, our MR analysis of gut microbiota–derived metabolites identified 3 significant associations with DLBCL risk. Two metabolites, 3-(4-hydroxyphenyl)lactate (OR = 0.174, 95% CI: 0.030–0.784; p = 0.023) and indolepropionate (OR = 0.296, 95% CI: 0.131–0.669; p = 0.003), were inversely associated with DLBCL risk, suggesting potential protective effects. In contrast, 7α-hydroxy-3-oxo-4-cholestenoate (7-HOCA) (OR = 9.561, 95% CI: 1.426–64.088; p = 0.020) exhibited a strong positive association with DLBCL risk, indicating a potential risk-promoting role (Table 2). BWMR validation confirmed 2 of these associations. Indolepropionate (OR = 0.256, 95% CI:

Table 1. The causal relationship estimation between gut microbiota and diffuse large B-cell lymphoma (DLBCL)

Gut microbiota (exposure)	Number of SNPs	β	p-value	OR (95% CI)	p-value for heterogeneity test	p-value for intercept	p-value for MR-PRESSO
Alistipes							
IVW	13	–0.652	0.013	0.521 (0.311–0.873)	0.889	0.257	0.797
MR Egger	13	0.834	0.525	2.302 (0.190–27.832)	0.928	–	–
Weighted median	13	–0.588	0.088	0.556 (0.283–1.092)	–	–	–
Simple mode	13	–0.498	0.395	0.608 (0.201–1.840)	–	–	–
Weighted mode	13	–0.515	0.369	0.597 (0.202–1.767)	–	–	–
BWMR	13	–0.557	0.036	0.573 (0.341–0.964)	–	–	–
Biophila							
IVW	13	0.575	0.031	1.777 (1.053–3.0)	0.121	0.659	0.089
MR Egger	13	1.181	0.405	3.256 (0.225–47.225)	0.095	–	–
Weighted median	13	0.827	0.012	2.286 (1.192–4.383)	–	–	–
Simple mode	13	1.194	0.092	3.200 (0.870–12.517)	–	–	–
Weighted mode	13	1.183	0.091	3.266 (1.019–10.468)	–	–	–
BWMR	13	0.696	0.005	2.005 (1.238–3.248)	–	–	–
Desulfovibrionaceae							
IVW	10	0.457	0.049	1.579 (1.003–2.487)	0.701	0.271	0.485
MR Egger	10	1.058	0.095	2.881 (0.964–8.615)	0.760	–	–
Weighted median	10	0.468	0.132	1.077 (0.869–2.936)	–	–	–
Simple mode	10	0.412	0.412	1.350 (0.591–3.856)	–	–	–
Weighted mode	10	0.429	0.308	1.206 (0.706–3.340)	–	–	–
BWMR	10	0.294	0.212	1.342 (0.846–2.130)	–	–	–
Ruminococcaceae UCG011							
IVW	8	–0.289	0.034	0.749 (0.574–0.978)	0.987	0.485	0.973
MR Egger	8	–0.785	0.293	0.456 (0.120–1.732)	0.983	–	–
Weighted median	8	–0.295	0.080	0.745 (0.535–1.036)	–	–	–
Simple mode	8	–0.344	0.216	0.709 (0.432–1.163)	–	–	–
Weighted mode	8	–0.364	0.222	0.695 (0.408–1.184)	–	–	–
BWMR	8	–0.291	0.04	0.747 (0.565–0.987)	–	–	–

SNPs – single nucleotide polymorphisms; OR – odds ratio; 95% CI – 95% confidence interval; IVW – inverse variance weighted; BWMR – Bayesian weighted Mendelian randomization.

0.100–0.650; p = 0.004) maintained its inverse association with DLBCL risk, whereas 7-HOCA (OR = 10.577, 95% CI: 1.275–87.729; p = 0.029) demonstrated an even stronger positive association. However, 3-(4-hydroxyphenyl)lactate (OR = 0.230, 95% CI: 0.040–1.314; p = 0.098) did not retain statistical significance in the BWMR analysis and was therefore not considered in further interpretation (Table 2). Scatter plots depicting the significant metabolite–DLBCL associations identified through BWMR analysis are presented in Fig. 2D–E. Forest plots visually summarize all significant microbiota–DLBCL causal relationships (Supplementary Fig. 1). Funnel plots demonstrated symmetrical distributions of causal estimates, indicating minimal evidence of directional pleiotropy that could bias the results (Supplementary Fig. 2).

Sensitivity analysis

Sensitivity analyses consistently supported the robustness of our findings. Cochran's Q test revealed no significant heterogeneity among the selected IVs (Tables 1,2). Additionally, the MR-Egger intercept test provided no evidence of significant horizontal pleiotropy. The MR-PRESSO global test (p > 0.05) identified no outlier variants among the gut microbial taxa, microbiota-derived metabolites, or DLBCL associations, further supporting the absence of horizontal pleiotropy (Tables 1,2). Finally, the leave-one-out analysis confirmed the stability of the estimates, demonstrating that no individual variant exerted a disproportionate influence on the causal associations (Supplementary Fig. 3).

Table 2. The causal relationship estimation between gut microbiota-derived metabolites and diffuse large B-cell lymphoma (DLBCL)

Metabolite (exposure)	Number of SNPs	β	p-value	OR (95% CI)	p-value for heterogeneity test	p-value for intercept	p-value for MR-PRESSO
3-(4-hydroxyphenyl)lactate							
IVW	22	−1.749	0.023	0.174 (0.030–0.784)	0.601	0.764	0.561
MR Egger	22	−2.269	0.133	0.103 (0.003–4.043)	0.544	–	–
Weighted median	22	−1.67	0.017	0.188 (0.021–1.682)	–	–	–
Simple mode	22	−2.601	0.188	0.074 (0.001–4.534)	–	–	–
Weighted mode	22	−3.011	0.2	0.049 (0.001–3.616)	–	–	–
BWMR	22	−1.47	0.098	0.23 (0.04–1.314)	–	–	–
7-HOCA							
IVW	15	2.258	0.02	9.561 (1.426–64.088)	0.423	0.561	0.455
MR Egger	15	3.772	0.190	43.47 (0.208–9140.125)	0.375	–	–
Weighted median	15	1.807	0.189	6.092 (0.411–90.161)	–	–	–
Simple mode	15	0.616	0.790	1.851 (0.022–159.266)	–	–	–
Weighted mode	15	1.527	0.484	4.604 (0.071–296.764)	–	–	–
BWMR	15	2.359	0.029	10.577 (1.275–87.729)	–	–	–
Indolepropionate							
IVW	16	−1.217	0.003	0.296 (0.131–0.669)	0.932	0.729	0.914
MR Egger	16	−0.958	0.273	0.384 (0.074–1.990)	0.906	–	–
Weighted median	16	−1.05	0.104	0.350 (0.099–1.239)	–	–	–
Simple mode	16	−1.815	0.116	0.163 (0.019–1.378)	–	–	–
Weighted mode	16	−0.86	0.235	0.423 (0.108–1.654)	–	–	–
BWMR	16	−1.364	0.004	0.256 (0.1–0.65)	–	–	–

SNPs – single nucleotide polymorphisms; OR – odds ratio; 95% CI – 95% confidence interval; IVW – inverse variance weighted; BWMR – Bayesian weighted Mendelian randomization; 7-HOCA – 7α-hydroxy-3-oxo- 4-cholestenoate.

Reverse MR results

In the reverse MR analysis evaluating DLBCL as exposure and gut microbiota as outcome, we initially identified 12 IVs, excluding those with weak instrument effects. Using IVW as the primary statistical method, DLBCL was found to be associated with a higher abundance of *Anaerofilum* (OR = 1.087, 95% CI: 1.008–1.173, p = 0.031) and a lower abundance of Deltaproteobacteria (OR = 0.959, 95% CI: 0.922–0.997, p = 0.037), *Desulfovibrionales* (OR = 0.959, 95% CI: 0.922–0.998, p = 0.041), Desulfovibrionaceae (OR = 0.960, 95% CI: 0.923–0.999, p = 0.045), Oxalobacteraceae (OR = 0.914, 95% CI: 0.843–0.992, p = 0.031), and *Oxalobacter* (OR = 0.909, 95% CI: 0.837–0.988, p = 0.024) (Table 3). The BWMR analysis provided further validation of the causal relationships between DLBCL and specific gut microbial taxa. This robust approach confirmed significant associations of DLBCL with Deltaproteobacteria (OR = 0.958, 95% CI: 0.920–0.999, p = 0.042), *Desulfovibrionales* (OR = 0.959, 95% CI: 0.920–0.999, p = 0.046), Oxalobacteraceae (OR = 0.911, 95% CI: 0.838–0.990, p = 0.027), *Anaerofilum* (OR = 1.091, 95% CI: 1.008–1.181, p = 0.030), and *Oxalobacter* (OR = 0.905, 95% CI: 0.832–0.986, p = 0.022). However, the association with Desulfovibrionaceae (OR = 0.960, 95% CI: 0.921–1.001, p = 0.051) narrowly missed the statistical significance threshold and was consequently excluded from final interpretation. Scatter plots of SNP effects supported the causal associations between DLBCL risk and gut microbiota abundance, as shown in Supplementary Fig. 4.

Forest plots demonstrated significant effects of DLBCL on specific gut microbial taxa in the reverse MR analysis (Supplementary Fig. 5). Funnel plots derived from the reverse MR analysis demonstrated a symmetrical distribution of variant effects, suggesting a low likelihood of directional pleiotropy (Supplementary Fig. 6). Importantly, sensitivity analyses performed for the reverse MR findings provided no evidence of significant heterogeneity or horizontal pleiotropy, with all relevant statistics summarized in Table 3. The leave-one-out analysis further confirmed the stability of the estimates, indicating that no single IV exerted a disproportionate influence on the causal effect estimates (Supplementary Fig. 7).

Discussion

In this study, we applied MR to systematically investigate the causal relationships between gut microbial features, microbiota-derived metabolites, and DLBCL risk.

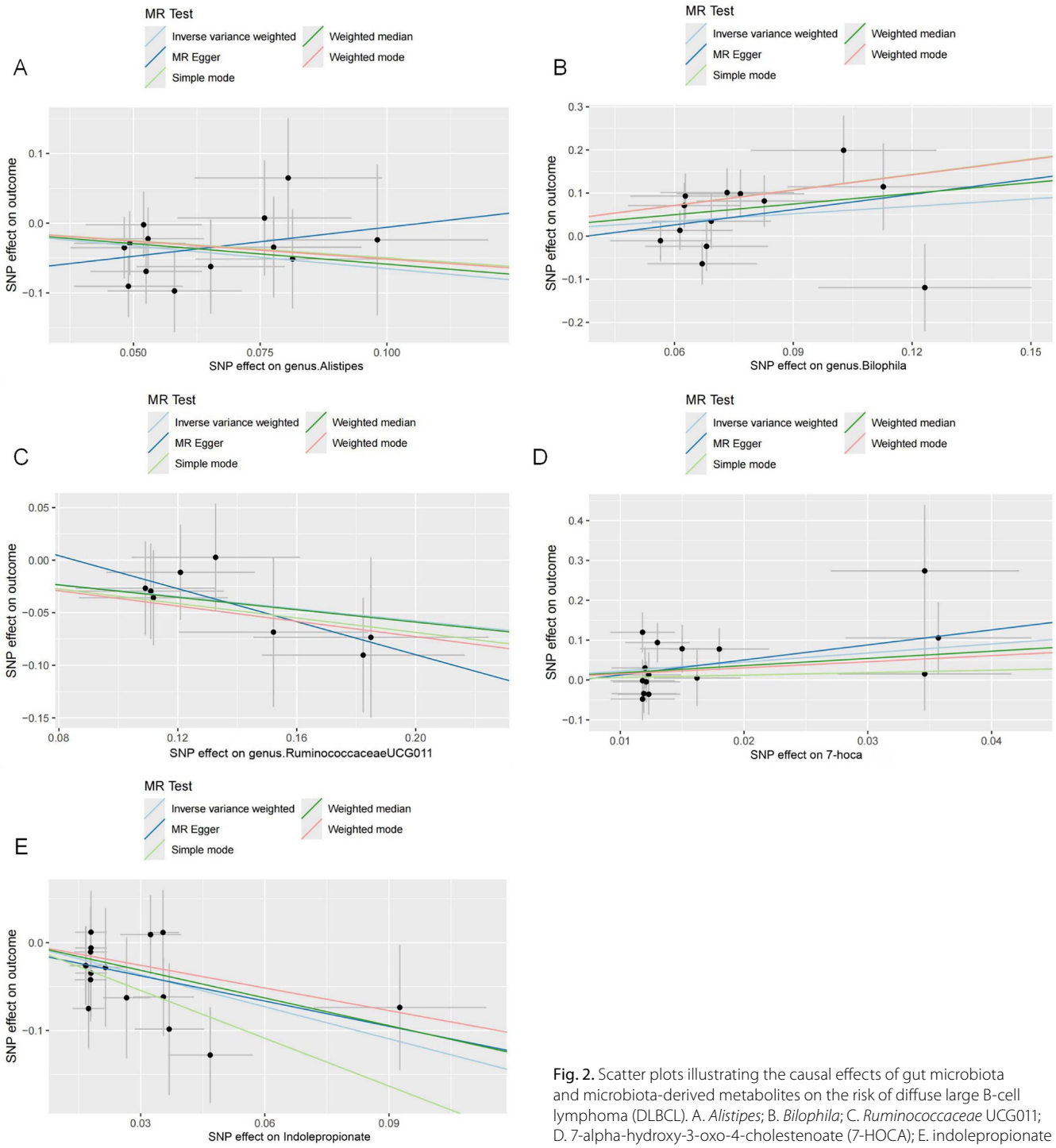

Fig. 2. Scatter plots illustrating the causal effects of gut microbiota and microbiota-derived metabolites on the risk of diffuse large B-cell lymphoma (DLBCL). A. *Alistipes*; B. *Bilophila*; C. *Ruminococcaceae* UCG011; D. 7-alpha-hydroxy-3-oxo-4-cholestenoate (7-HOCA); E. indolepropionate

The findings identified 3 bacterial genera – *Alistipes*, *Ruminococcaceae* UCG011, and *Bilophila* – along with 2 microbiota-derived metabolites, indolepropionate and 7-HOCA, that demonstrated significant causal associations with DLBCL risk. Furthermore, reverse MR analysis suggested that DLBCL may reciprocally influence gut microbial composition, with putative causal effects observed for 1 bacterial class (Deltaproteobacteria), 1 order (*Desulfovibrionales*), 1 family (Oxalobacteraceae), and 2 genera (*Anaerofilum* and *Oxalobacter*). The gut microbiota, comprising more than 1,000 taxonomic units residing in the intestinal tract, is increasingly recognized as a vital "virtual organ" due to its structural complexity and partially heritable characteristics. This microbial community plays a pivotal role in maintaining host physiological homeostasis through diverse direct and indirect mechanisms.[40] Growing evidence suggests that perturbations in gut microbial ecology contribute to the pathogenesis of various diseases, including hematological malignancies.[41,42] Recent studies have further implicated gut microbiota dysbiosis in lymphomagenesis and disease progression.[43,44] Supporting this connection, Lin et al. reported

Table 3. The causal relationship estimation between diffuse large B-cell lymphoma (DLBCL) and gut microbiota

Gut microbiota (outcome)	Number of SNPs	β	p-value	OR (95% CI)	p-value for heterogeneity test	p-value for intercept	p-value for MR-PRESSO
Deltaproteobacteria							
IVW	7	–0.042	0.037	0.959 (0.922–0.997)	0.889	0.508	0.907
MR Egger	7	–0.118	0.326	0.889 (0.719–1.099)	0.876	–	–
Weighted median	7	–0.054	0.030	0.947 (0.902–0.995)	–	–	–
Simple mode	7	–0.058	0.171	0.944 (0.877–1.015)	–	–	–
Weighted mode	7	–0.058	0.137	0.944 (0.884–1.008)	–	–	–
BWMR	7	0.043	0.042	0.958 (0.920–0.999)	–	–	–
Desulfovibrionales							
IVW	7	–0.041	0.041	0.959 (0.922–0.998)	0.889	0.257	0.8
MR Egger	7	–0.120	0.316	0.887 (0.717–1.096)	0.928	–	–
Weighted median	7	–0.054	0.027	0.947 (0.903–0.994)	–	–	–
Simple mode	7	–0.058	0.170	0.944 (0.877–1.015)	–	–	–
Weighted mode	7	–0.057	0.161	0.945 (0.881–1.013)	–	–	–
BWMR	7	–0.042	0.046	0.959 (0.920–0.999)	–	–	–
Desulfovibrionaceae							
IVW	7	–0.041	0.045	0.960 (0.923–0.999)	0.88	0.506	0.893
MR Egger	7	–0.117	0.330	0.890 (0.720–1.010)	0.865	–	–
Weighted median	7	–0.053	0.038	0.948 (0.903–0.996)	–	–	–
Simple mode	7	–0.057	0.169	0.945 (0.882–1.012)	–	–	–
Weighted mode	7	–0.056	0.163	0.946 (0.886–1.010)	–	–	–
BWMR	7	–0.041	0.051	0.960 (0.921–1.0001)	–	–	–
Oxalobacteraceae							
IVW	7	–0.090	0.031	0.914 (0.843–0.992)	0.188	0.930	0.211
MR Egger	7	–0.068	0.792	0.935 (0.581–1.504)	0.120	–	–
Weighted median	7	–0.069	0.172	0.933 (0.845–1.031)	–	–	–
Simple mode	7	–0.068	0.450	0.934 (0.793–1.101)	–	–	–
Weighted mode	7	–0.129	0.137	0.879 (0.759–1.018)	–	–	–
BWMR	7	–0.093	0.027	0.911 (0.838–0.990)	–	–	–
Anaerofilum							
IVW	7	0.083	0.031	1.087 (1.008–1.173)	0.279	0.940	0.333
MR Egger	7	0.101	0.675	1.106 (0.708–1.727)	0.188	–	–
Weighted median	7	0.120	0.011	1.128 (1.028–1.238)	–	–	–
Simple mode	7	0.143	0.091	1.154 (1.004–1.326)	–	–	–
Weighted mode	7	0.138	0.086	1.147 (1.006–1.308)	–	–	–
BWMR	7	0.087	0.03	1.091 (1.008–1.181)	–	–	–
Oxalobacter							
IVW	7	–0.095	0.024	0.909 (0.837–0.988)	0.222	0.995	0.249
MR Egger	7	–0.093	0.722	0.911 (0.560–1.482)	0.144	–	–
Weighted median	7	–0.061	0.244	0.940 (0.848–1.043)	–	–	–
Simple mode	7	–0.010	0.916	0.990 (0.816–1.200)	–	–	–
Weighted mode	7	–0.008	0.938	0.992 (0.822–1.198)	–	–	–
BWMR	7	–0.099	0.022	0.905 (0.832–0.986)	–	–	–

SNPs – single nucleotide polymorphisms; OR – odds ratio; 95% CI – 95% confidence interval; IVW – inverse variance weighted; BWMR – Bayesian weighted Mendelian randomization.

distinct gut microbiota profiles in untreated DLBCL patients, characterized by significantly elevated abundances of Proteobacteria, *Escherichia–Shigella*, *Roseburia*, and *Alistipes* compared with healthy controls.[18] In contrast, Li et al. observed a significant depletion of *Roseburia* in DLBCL patients.[20] Further clinical observations

indicated that patients experiencing treatment-related adverse events exhibited higher levels of Enterobacteriaceae, whereas those without adverse events showed relative enrichment of Prevotellaceae and Oscillospiraceae.[22] Moreover, a significant difference in Enterobacteriaceae abundance was observed between patients with disease relapse or progression and those in remission.[22] Recent investigations have identified significant microbial shifts in treatment-naïve patients, characterized by increased levels of Bacteroidetes and decreased levels of Firmicutes compared with healthy controls.[43] Firmicutes, particularly members of the families Ruminococcaceae and Lachnospiraceae, are major butyrate producers in the human colon.[45,46] In our study, *Ruminococcaceae* UCG011, a butyrate-producing bacterial genus, was inversely associated with DLBCL risk (OR = 0.749). This protective association suggests potential anti-lymphoma effects that may operate through multiple butyrate-mediated mechanisms. As the primary short-chain fatty acid (SCFA) generated through microbial fermentation of dietary fiber, butyrate serves as a key energy source for colonocytes while also modulating immune responses and enhancing intestinal barrier integrity.[47] Moreover, Wei et al. demonstrated that butyrate exerts potent anti-tumor effects by functioning as a histone deacetylase (HDAC) inhibitor, thereby promoting histone acetylation and inducing apoptosis of malignant cells through epigenetic modulation of gene expression pathways.[24] The anti-tumor effects of butyrate may be particularly relevant in DLBCL, given the characteristic overexpression of HDAC isoforms observed in this malignancy.[48,49] Similar HDAC-mediated oncogenic processes have been reported across multiple malignancies, in which butyrate's HDAC-inhibitory activity promotes tumor-suppressive histone acetylation and apoptosis.[50,51]

Existing evidence also indicates that butyrate regulates key oncogenic pathways including mitochondrial and extrinsic apoptosis, G protein-coupled receptor (GPR41/43/109a) signaling, Wnt signaling, and protein kinase C pathway.[52] Particularly relevant to lymphomagenesis, Lu et al. reported that butyrate-producing *Eubacterium rectale* suppresses tumor necrosis factor (TNF) production and subsequent TLR4/MyD88/NF-κB activation in B cells, which may contribute to reduced lymphoma incidence.[23] Our current analysis did not detect significant associations of *E. rectale* with DLBCL risk, potentially due to limited sample size. However, the robust association with *Ruminococcaceae* UCG011 warrants future investigation into its specific mechanisms of action, particularly its potential to modulate these reported butyrate-sensitive pathways in B-cell malignancies.

Alistipes, a recently identified genus of anaerobic bacteria, predominantly colonizes the human gastrointestinal tract but has also been identified in extraintestinal sites including the brain, bloodstream, and gut periphery.[53] This bacterial genus demonstrates complex disease-modulating properties, with studies reporting both protective and pathogenic associations. Several studies have reported that *Alistipes* exerts protective effects against colitis.[54] In patients with liver cirrhosis, *Alistipes* abundance declines progressively from the compensated to the decompensated stage.[55,56] The onset and severity of liver fibrosis have been associated with reduced *Alistipes* populations. The observed antifibrotic effects may be mediated through *Alistipes* production of propionate and acetate, with the latter exhibiting well-documented anti-inflammatory properties.[57,58] Additionally, emerging evidence indicates complex, context-dependent roles for *Alistipes* in cancer biology. While elevated *Alistipes* abundance has demonstrated protective effects against hepatocellular carcinoma (HCC) progression, potentially mediated through the suppression of hepatic T helper 17 cells,[59] other studies suggest this genus may promote carcinogenesis in colorectal cancer via IL-6/STAT3 pathway activation.[60] Our findings revealed a similarly protective association between *Alistipes* and DLBCL risk, which may be mediated through immunomodulatory mechanisms analogous to those observed in hepatic malignancies. However, the precise pathways underlying *Alistipes*–DLBCL interactions require further mechanistic investigation.

Moreover, our MR analysis revealed a significant positive association between *Bilophila* and the risk of DLBCL. The anaerobic genus *Bilophila* has been implicated in diverse pathological conditions, including abscesses, appendicitis, colitis, and Parkinson's disease.[61] Studies have demonstrated that *Bilophila* generates hydrogen sulfide (H_2S), a gaseous metabolite that significantly compromises intestinal barrier function. This disruption facilitates direct contact between harmful substances or bacteria and epithelial surfaces, thereby impairing immune responses, activating inflammation, and ultimately promoting colorectal tumorigenesis.[62,63] Furthermore, evidence also suggests that *Bilophila* exhibits inhibitory effects on butyrate-producing gut microbiota, simultaneously affecting both microbial balance and host physiology.[64] Given the established protective role of butyrate against DLBCL, it is plausible that *Bilophila* may contribute to DLBCL pathogenesis through butyrate depletion mechanisms. However, the precise nature of this relationship remains to be elucidated, as no prior studies have directly investigated *Bilophila*–DLBCL associations.

The gut microbiota serves as a key biosynthetic organ for circulating metabolites, generating diverse small molecules that systemically regulate host physiology through multiple mechanisms. Emerging evidence links dysregulation of these microbial metabolic pathways to various disease states.[65,66] As previously discussed, elevated levels of butyrate have been associated with reduced lymphoma burden, whereas the loss of butyrate-producing bacteria may diminish these beneficial effects.[24] Moreover, this relationship is further supported by observations in NK/T-cell lymphoma patients, who exhibit significantly reduced levels of both butyrate and its primary producer *Faecalibacterium prausnitzii*. Butyrate is hypothesized to inhibit

tumor progression by activating SOCS1 and suppressing the JAK–STAT signaling pathway.[67] Building upon our initial findings, we conducted a comprehensive investigation of the causal relationships between gut microbiota-derived metabolites and DLBCL risk. Our analysis identified indolepropionate, a microbial metabolite generated from dietary tryptophan catabolism,[68] as a potentially protective factor for DLBCL. This compound demonstrates multifaceted biological activity, including the stimulation of interleukin (IL)-10 secretion from bone marrow-derived macrophages to exert potent anti-inflammatory effects.[69] Another study demonstrated that indolepropionate attenuates intestinal inflammation by suppressing interferon gamma (IFN-γ), TNF-α, and IL-1β through its action as an aryl hydrocarbon receptor (AHR) ligand that promotes IL-22 production.[68] Indolepropionate has also been reported to exhibit anti-tumor effects by inhibiting epithelial-mesenchymal transition, enhancing anti-tumor immunity through upregulation of both AHR and pregnane X receptor (PXR) pathways, and functioning as a free radical scavenger against oxidative DNA damage induced by carcinogens like free iron and Cr(III).[70–72] The convergence of these anticancer properties with our MR findings suggests its potential relevance to DLBCL prevention and treatment, although the specific mechanisms in lymphoid malignancies remain to be fully elucidated.

In contrast to well-characterized microbial metabolites, the pathological significance of 7-HOCA remains poorly understood. A recent study reported elevated levels of 7-HOCA in patients with hepatitis and liver cancer and demonstrated that 7-HOCA induces DNA damage and promotes tumorigenesis in non-alcoholic fatty liver disease (NAFLD).[73] In our MR analyses, 7-HOCA was identified as a potential risk factor for DLBCL, providing a compelling rationale for further investigations into the molecular mechanisms through which 7-HOCA may contribute to lymphomagenesis.

This study has several methodological strengths compared with previous research. We employed a MR design to infer causal relationships between gut microbiota, microbiota-derived metabolites, and DLBCL. Bidirectional MR analyses were conducted using large-scale GWAS datasets to comprehensively evaluate these associations. Single nucleotide polymorphisms were selected as instrumental variables to emulate the random allocation of genetic variants. According to Mendel's laws, these variants are randomly assigned at conception and are generally independent of environmental confounders. As highlighted by Ference et al.,[74] this intrinsic property enables MR to estimate causal effects of exposures on disease outcomes with reduced confounding. By serving as proxies for long-term exposure, SNPs facilitate more robust causal inference. To assess potential horizontal pleiotropy, we applied both MR-Egger regression and MR-PRESSO. Finally, the robustness of our findings was further supported through complementary analyses using BWMR.

Limitations of the study

Despite its strengths, this study has several limitations that warrant consideration. First, the GWAS data on gut microbiota and metabolites were predominantly derived from European cohorts, and the DLBCL dataset also consisted exclusively of individuals of European ancestry. Consequently, our findings may be susceptible to population stratification bias and may not be generalizable to non-European populations. Second, the absence of clinical subtyping data precluded important stratified analyses, including the evaluation of differences according to cell-of-origin classification (germinal center B-cell (GCB) vs non-GCB subtypes) or the presence of gastrointestinal involvement. Finally, the resolution of the gut microbiota data was limited to the genus level, and the metabolite dataset was incomplete, thereby constraining more in-depth mechanistic exploration. Future studies incorporating more comprehensive and higher-resolution datasets are warranted to validate and refine the inferred causal relationships between gut microbiota and DLBCL.

Conclusions

In summary, our findings provide evidence supporting potential causal relationships between gut microbiota, microbiota-derived metabolites, and DLBCL, offering new insights into DLBCL pathogenesis and informing future diagnostic and therapeutic strategies. However, given the limitations of this study, further experimental and clinical investigations are warranted to more comprehensively elucidate the roles of gut microbiota and their metabolites in DLBCL development.

Supplementary data

The supplementary materials are available at https://doi.org/10.5281/zenodo.17047566. The package contains the following files:

Supplementary Fig. 1. The forest plots of the causal effects of gut microbiota and derived metabolites on the risk of DLBCL.

Supplementary Fig. 2. The funnel plots of the causal effects of gut microbiota and derived metabolites on the risk of DLBCL.

Supplementary Fig. 3. The leave-one-out analyses of the causal effects of gut microbiota and derived metabolites on the risk of DLBCL.

Supplementary Fig. 4. The scatter plots of the causal effects of DLBCL on the risk of gut microbiota.

Supplementary Fig. 5. The forest plots of DLBCL on the risk of gut microbiota.

Supplementary Fig. 6. The funnel plots of DLBCL on the risk of gut microbiota.

Supplementary Fig. 7. The leave-one-out analyses of DLBCL on the risk of gut microbiota.

Data Availability Statement

All datasets used in this study are publicly available. Gut microbiota GWAS data were obtained from the MiBioGen consortium (https://mibiogen.gcc.rug.nl), metabolite GWAS data from the TwinsUK and KORA studies annotated via the Human Metabolome Database (https://hmdb.ca), and DLBCL summary statistics from the FinnGen consortium (https://www.finngen.fi/en, release R10, December 2023). The code for Mendelian randomization analyses is available in Zenodo at https://doi.org/10.5281/zenodo.17047705.

Consent for publication

Not applicable.

Use of AI and AI-assisted technologies

Not applicable.

ORCID iDs

Ganyu Feng https://orcid.org/0009-0000-7063-1025

References

1. Grulich AE, Vajdic CM. The epidemiology of non-Hodgkin lymphoma. *Pathology*. 2005;37(6):409–419. doi:10.1080/00313020500370192
2. Chu Y, Liu Y, Fang X, et al. The epidemiological patterns of non-Hodgkin lymphoma: Global estimates of disease burden, risk factors, and temporal trends. *Front Oncol*. 2023;13:1059914. doi:10.3389/fonc.2023.1059914
3. Li S, Young KH, Medeiros LJ. Diffuse large B-cell lymphoma. *Pathology*. 2018;50(1):74–87. doi:10.1016/j.pathol.2017.09.006
4. Tilly H, Gomes Da Silva M, Vitolo U, et al. Diffuse large B-cell lymphoma (DLBCL): ESMO Clinical Practice Guidelines for diagnosis, treatment and follow-up. *Ann Oncol*. 2015;26:v116–v125. doi:10.1093/annonc/mdv304
5. Martelli M, Ferreri AJM, Agostinelli C, Di Rocco A, Pfreundschuh M, Pileri SA. Diffuse large B-cell lymphoma. *Crit Rev Oncol Hematol*. 2013;87(2):146–171. doi:10.1016/j.critrevonc.2012.12.009
6. Shi Z, Zhang M. Emerging roles for the gut microbiome in lymphoid neoplasms. *Clin Med Insights Oncol*. 2021;15:11795549211024197. doi:10.1177/11795549211024197
7. Upadhyay Banskota S, Skupa SA, El-Gamal D, D'Angelo CR. Defining the role of the gut microbiome in the pathogenesis and treatment of lymphoid malignancies. *Int J Mol Sci*. 2023;24(3):2309. doi:10.3390/ijms24032309
8. Ley RE, Turnbaugh PJ, Klein S, Gordon JI. Human gut microbes associated with obesity. *Nature*. 2006;444(7122):1022–1023. doi:10.1038/4441022a
9. Thursby E, Juge N. Introduction to the human gut microbiota. *Biochem J*. 2017;474(11):1823–1836. doi:10.1042/BCJ20160510
10. Den Besten G, Van Eunen K, Groen AK, Venema K, Reijngoud DJ, Bakker BM. The role of short-chain fatty acids in the interplay between diet, gut microbiota, and host energy metabolism. *J Lipid Res*. 2013;54(9):2325–2340. doi:10.1194/jlr.R036012
11. Bäumler AJ, Sperandio V. Interactions between the microbiota and pathogenic bacteria in the gut. *Nature*. 2016;535(7610):85–93. doi:10.1038/nature18849
12. Natividad JMM, Verdu EF. Modulation of intestinal barrier by intestinal microbiota: Pathological and therapeutic implications. *Pharmacol Res*. 2013;69(1):42–51. doi:10.1016/j.phrs.2012.10.007
13. Gensollen T, Iyer SS, Kasper DL, Blumberg RS. How colonization by microbiota in early life shapes the immune system. *Science*. 2016;352(6285):539–544. doi:10.1126/science.aad9378
14. Guevara-Ramírez P, Cadena-Ullauri S, Paz-Cruz E, Tamayo-Trujillo R, Ruiz-Pozo VA, Zambrano AK. Role of the gut microbiota in hematologic cancer. *Front Microbiol*. 2023;14:1185787. doi:10.3389/fmicb.2023.1185787
15. Meng C, Bai C, Brown TD, Hood LE, Tian Q. Human gut microbiota and gastrointestinal cancer. *Genomics Proteomics Bioinformatics*. 2018;16(1):33–49. doi:10.1016/j.gpb.2017.06.002
16. Yu X, Jiang W, Kosik RO, et al. Gut microbiota changes and its potential relations with thyroid carcinoma. *J Adv Res*. 2022;35:61–70. doi:10.1016/j.jare.2021.04.001
17. Zhao Y, Liu Y, Li S, et al. Role of lung and gut microbiota on lung cancer pathogenesis. *J Cancer Res Clin Oncol*. 2021;147(8):2177–2186. doi:10.1007/s00432-021-03644-0
18. Lin Z, Mao D, Jin C, et al. The gut microbiota correlate with the disease characteristics and immune status of patients with untreated diffuse large B-cell lymphoma. *Front Immunol*. 2023;14:1105293. doi:10.3389/fimmu.2023.1105293
19. Nowicka A, Gil L. Microbial metabolomics in acute myeloid leukemia: From pathogenesis to treatment [published online as ahead of print on October 21, 2025]. *Adv Clin Exp Med*. 2024. doi:10.17219/acem/191559
20. Yuan L, Wang W, Zhang W, et al. Gut microbiota in untreated diffuse large B cell lymphoma patients. *Front Microbiol*. 2021;12:646361. doi:10.3389/fmicb.2021.646361
21. Zhang Y, Han S, Xiao X, et al. Integration analysis of tumor metagenome and peripheral immunity data of diffuse large-B cell lymphoma. *Front Immunol*. 2023;14:1146861. doi:10.3389/fimmu.2023.1146861
22. Yoon SE, Kang W, Choi S, et al. The influence of microbial dysbiosis on immunochemotherapy-related efficacy and safety in diffuse large B-cell lymphoma. *Blood*. 2023;141(18):2224–2238. doi:10.1182/blood.2022018831
23. Lu H, Xu X, Fu D, et al. Butyrate-producing *Eubacterium rectale* suppresses lymphomagenesis by alleviating the TNF-induced TLR4/MyD88/NF-κB axis. *Cell Host Microbe*. 2022;30(8):1139–1150.e7. doi:10.1016/j.chom.2022.07.003
24. Wei W, Sun W, Yu S, Yang Y, Ai L. Butyrate production from high-fiber diet protects against lymphoma tumor. *Leuk Lymphoma*. 2016;57(10):2401–2408. doi:10.3109/10428194.2016.1144879
25. Rinninella E, Raoul P, Cintoni M, et al. What is the healthy gut microbiota composition? A changing ecosystem across age, environment, diet, and diseases. *Microorganisms*. 2019;7(1):14. doi:10.3390/microorganisms7010014
26. Emdin CA, Khera AV, Kathiresan S. Mendelian randomization. *JAMA*. 2017;318(19):1925. doi:10.1001/jama.2017.17219
27. Long Y, Tang L, Zhou Y, Zhao S, Zhu H. Causal relationship between gut microbiota and cancers: A two-sample Mendelian randomisation study. *BMC Med*. 2023;21(1):66. doi:10.1186/s12916-023-02761-6
28. Ma J, Li J, Jin C, et al. Association of gut microbiome and primary liver cancer: A two-sample Mendelian randomization and case–control study. *Liver Int*. 2023;43(1):221–233. doi:10.1111/liv.15466
29. Van Der Velde KJ, Imhann F, Charbon B, et al. MOLGENIS research: Advanced bioinformatics data software for non-bioinformaticians. *Bioinformatics*. 2019;35(6):1076–1078. doi:10.1093/bioinformatics/bty742
30. Li P, Wang H, Guo L, et al. Association between gut microbiota and preeclampsia-eclampsia: A two-sample Mendelian randomization study. *BMC Med*. 2022;20(1):443. doi:10.1186/s12916-022-02657-x
31. Pierce BL, Ahsan H, VanderWeele TJ. Power and instrument strength requirements for Mendelian randomization studies using multiple genetic variants. *Int J Epidemiol*. 2011;40(3):740–752. doi:10.1093/ije/dyq151
32. Burgess S, Butterworth A, Thompson SG. Mendelian randomization analysis with multiple genetic variants using summarized data. *Genet Epidemiol*. 2013;37(7):658–665. doi:10.1002/gepi.21758
33. Burgess S, Dudbridge F, Thompson SG. Combining information on multiple instrumental variables in Mendelian randomization: Comparison of allele score and summarized data methods. *Statist Med*. 2016;35(11):1880–1906. doi:10.1002/sim.6835
34. Bowden J, Davey Smith G, Burgess S. Mendelian randomization with invalid instruments: Effect estimation and bias detection through Egger regression. *Int J Epidemiol*. 2015;44(2):512–525. doi:10.1093/ije/dyv080

35. Bowden J, Davey Smith G, Haycock PC, Burgess S. Consistent estimation in Mendelian randomization with some invalid instruments using a weighted median estimator. *Genet Epidemiol*. 2016;40(4):304–314. doi:10.1002/gepi.21965
36. Hemani G, Zheng J, Elsworth B, et al. The MR-Base platform supports systematic causal inference across the human phenome. *eLife*. 2018;7:e34408. doi:10.7554/eLife.34408
37. Verbanck M, Chen CY, Neale B, Do R. Detection of widespread horizontal pleiotropy in causal relationships inferred from Mendelian randomization between complex traits and diseases. *Nat Genet*. 2018;50(5):693–698. doi:10.1038/s41588-018-0099-7
38. Hemani G, Tilling K, Davey Smith G. Orienting the causal relationship between imprecisely measured traits using GWAS summary data. *PLoS Genet*. 2017;13(11):e1007081. doi:10.1371/journal.pgen.1007081
39. Zhao J, Ming J, Hu X, Chen G, Liu J, Yang C. Bayesian weighted Mendelian randomization for causal inference based on summary statistics. *Bioinformatics*. 2020;36(5):1501–1508. doi:10.1093/bioinformatics/btz749
40. Baquero F, Nombela C. The microbiome as a human organ. *Clin Microbiol Infect*. 2012;18:2–4. doi:10.1111/j.1469-0691.2012.03916.x
41. Gagnière J. Gut microbiota imbalance and colorectal cancer. *World J Gastroenterol*. 2016;22(2):501. doi:10.3748/wjg.v22.i2.501
42. Lucas C, Barnich N, Nguyen H. Microbiota, inflammation and colorectal cancer. *Int J Mol Sci*. 2017;18(6):1310. doi:10.3390/ijms18061310
43. Diefenbach CS, Peters BA, Li H, et al. Microbial dysbiosis is associated with aggressive histology and adverse clinical outcome in B-cell non-Hodgkin lymphoma. *Blood Adv*. 2021;5(5):1194–1198. doi:10.1182/bloodadvances.2020003129
44. Yamamoto ML, Maier I, Dang AT, et al. Intestinal bacteria modify lymphoma incidence and latency by affecting systemic inflammatory state, oxidative stress, and leukocyte genotoxicity. *Cancer Res*. 2013;73(14):4222–4232. doi:10.1158/0008-5472.CAN-13-0022
45. Barcenilla A, Pryde SE, Martin JC, et al. Phylogenetic relationships of butyrate-producing bacteria from the human gut. *Appl Environ Microbiol*. 2000;66(4):1654–1661. doi:10.1128/AEM.66.4.1654-1661.2000
46. Louis P, Duncan SH, McCrae SI, Millar J, Jackson MS, Flint HJ. Restricted distribution of the butyrate kinase pathway among butyrate-producing bacteria from the human colon. *J Bacteriol*. 2004;186(7):2099–2106. doi:10.1128/JB.186.7.2099-2106.2004
47. Liu H, Wang J, He T, et al. Butyrate: A double-edged sword for health? *Adv Nutr*. 2018;9(1):21–29. doi:10.1093/advances/nmx009
48. Lee SH, Yoo C, Im S, Jung JH, Choi HJ, Yoo J. Expression of histone deacetylases in diffuse large B-cell lymphoma and its clinical significance. *Int J Med Sci*. 2014;11(10):994–1000. doi:10.7150/ijms.8522
49. Johnson DP, Spitz GS, Tharkar S, et al. HDAC1,2 inhibition impairs EZH2- and BBAP-mediated DNA repair to overcome chemoresistance in EZH2 gain-of-function mutant diffuse large B-cell lymphoma. *Oncotarget*. 2015;6(7):4863–4887. doi:10.18632/oncotarget.3120
50. Donohoe DR, Holley D, Collins LB, et al. A gnotobiotic mouse model demonstrates that dietary fiber protects against colorectal tumorigenesis in a microbiota- and butyrate-dependent manner. *Cancer Discov*. 2014;4(12):1387–1397. doi:10.1158/2159-8290.CD-14-0501
51. Stojanovic N, Hassan Z, Wirth M, et al. HDAC1 and HDAC2 integrate the expression of p53 mutants in pancreatic cancer. *Oncogene*. 2017;36(13):1804–1815. doi:10.1038/onc.2016.344
52. Chen J, Zhao KN, Vitetta L. Effects of intestinal microbial-elaborated butyrate on oncogenic signaling pathways. *Nutrients*. 2019;11(5):1026. doi:10.3390/nu11051026
53. Shkoporov AN, Chaplin AV, Khokhlova EV, et al. *Alistipes inops* sp. nov. and *Coprobacter secundus* sp. nov., isolated from human faeces. *Int J Syst Evol Microbiol*. 2015;65(Pt 12):4580–4588. doi:10.1099/ijsem.0.000617
54. Dziarski R, Park SY, Kashyap DR, Dowd SE, Gupta D. Pglyrp-regulated gut microflora *Prevotella falsenii*, *Parabacteroides distasonis* and *Bacteroides eggerthii* enhance and *Alistipes finegoldii* attenuates colitis in mice. *PLoS One*. 2016;11(1):e0146162. doi:10.1371/journal.pone.0146162
55. Iebba V, Guerrieri F, Di Gregorio V, et al. Combining amplicon sequencing and metabolomics in cirrhotic patients highlights distinctive microbiota features involved in bacterial translocation, systemic inflammation and hepatic encephalopathy. *Sci Rep*. 2018;8(1):8210. doi:10.1038/s41598-018-26509-y
56. Shao L, Ling Z, Chen D, Liu Y, Yang F, Li L. Disorganized gut microbiome contributed to liver cirrhosis progression: A meta-omics-based study. *Front Microbiol*. 2018;9:3166. doi:10.3389/fmicb.2018.03166
57. Oliphant K, Allen-Vercoe E. Macronutrient metabolism by the human gut microbiome: Major fermentation by-products and their impact on host health. *Microbiome*. 2019;7(1):91. doi:10.1186/s40168-019-0704-8
58. Parker BJ, Wearsch PA, Veloo ACM, Rodriguez-Palacios A. The genus *Alistipes*: Gut bacteria with emerging implications to inflammation, cancer, and mental health. *Front Immunol*. 2020;11:906. doi:10.3389/fimmu.2020.00906
59. Li J, Sung CYJ, Lee N, et al. Probiotics modulated gut microbiota suppresses hepatocellular carcinoma growth in mice. *Proc Natl Acad Sci U S A*. 2016;113(9):E1306-15. doi:10.1073/pnas.1518189113
60. Moschen AR, Gerner RR, Wang J, et al. Lipocalin 2 protects from inflammation and tumorigenesis associated with gut microbiota alterations. *Cell Host Microbe*. 2016;19(4):455–469. doi:10.1016/j.chom.2016.03.007
61. Burrichter AG, Dörr S, Bergmann P, et al. Bacterial microcompartments for isethionate desulfonation in the taurine-degrading human-gut bacterium *Bilophila wadsworthia*. *BMC Microbiol*. 2021;21(1):340. doi:10.1186/s12866-021-02386-w
62. Waqas M, Halim SA, Ullah A, et al. Multi-fold computational analysis to discover novel putative inhibitors of isethionate sulfite-lyase (Isla) from *Bilophila wadsworthia*: Combating colorectal cancer and inflammatory bowel diseases. *Cancers (Basel)*. 2023;15(3):901. doi:10.3390/cancers15030901
63. Yazici C, Wolf PG, Kim H, et al. Race-dependent association of sulfidogenic bacteria with colorectal cancer. *Gut*. 2017;66(11):1983–1994. doi:10.1136/gutjnl-2016-313321
64. Natividad JM, Lamas B, Pham HP, et al. Bilophila wadsworthia aggravates high fat diet induced metabolic dysfunctions in mice. *Nat Commun*. 2018;9(1):2802. doi:10.1038/s41467-018-05249-7
65. Yue X, Zhou H, Wang S, Chen X, Xiao H. Gut microbiota, microbiota-derived metabolites, and graft-versus-host disease. *Cancer Med*. 2024;13(3):e6799. doi:10.1002/cam4.6799
66. D'Angelo CR, Sudakaran S, Callander NS. Clinical effects and applications of the gut microbiome in hematologic malignancies. *Cancer*. 2021;127(5):679–687. doi:10.1002/cncr.33400
67. Shi Z, Li M, Zhang C, et al. Butyrate-producing *Faecalibacterium prausnitzii* suppresses natural killer/T-cell lymphoma by dampening the JAK-STAT pathway. *Gut*. 2025;74(4):557–570. doi:10.1136/gutjnl-2024-333530
68. Jiang H, Chen C, Gao J. Extensive summary of the important roles of indole propionic acid, a gut microbial metabolite in host health and disease. *Nutrients*. 2022;15(1):151. doi:10.3390/nu15010151
69. Wlodarska M, Luo C, Kolde R, et al. Indoleacrylic acid produced by commensal *Peptostreptococcus* species suppresses inflammation. *Cell Host Microbe*. 2017;22(1):25–37.e6. doi:10.1016/j.chom.2017.06.007
70. Sári Z, Mikó E, Kovács T, et al. Indolepropionic acid, a metabolite of the microbiome, has cytostatic properties in breast cancer by activating AHR and PXR receptors and inducing oxidative stress. *Cancers (Basel)*. 2020;12(9):2411. doi:10.3390/cancers12092411
71. Qi W, Reiter RJ, Tan D, Manchester LC, Siu AW, Garcia JJ. Increased levels of oxidatively damaged DNA induced by chromium(III) and H_2O_2: protection by melatonin and related molecules. *J Pineal Res*. 2000;29(1):54–61. doi:10.1034/j.1600-079X.2000.290108.x
72. Karbownik M, Reiter RJ, Garcia JJ, et al. Indole-3-propionic acid, a melatonin-related molecule, protects hepatic microsomal membranes from iron-induced oxidative damage: Relevance to cancer reduction. *J Cell Biochem*. 2001;81(3):507–513. PMID:11255233.
73. Nikolaou N, Arvaniti A, Sanna F, et al. AKR1D1 knockdown identifies 7[alpha]-hydroxy-3-oxo-4-cholestenoic acid (7-HOCA) as a driver of metabolic dysfunction and hepatocellular cancer risk in patients with non-alcoholic fatty liver disease (NAFLD). *Endocr Abstracts*. 2022;81:Y18. doi:10.1530/endoabs.81.YI8
74. Ference BA, Holmes MV, Smith GD. Using Mendelian randomization to improve the design of randomized trials. *Cold Spring Harb Perspect Med*. 2021;11(7):a040980. doi:10.1101/cshperspect.a040980